Colloid Polym Sci (2004) 283: 145–153
DOI 10.1007/s00396-004-1110-7

ORIGINAL CONTRIBUTION

Saeed Rastegar
Naser Mohammadi
Reza Bagheri

Development of co-continuous morphology in epoxy poly(methyl methacrylate) (PMMA) blends cured by mixtures of phase-separating and non-phase-separating curing agents

Received: 10 November 2003
Accepted: 18 March 2003
Published online: 25 May 2004

S. Rastegar · N. Mohammadi (✉)
Loghman Fundamental Research Group,
Polymer Engineering Department,
Amirkabir University of Technology,
P.O. Box 15875, 4413 Tehran, Iran
E-mail: mohamadi@cic.aut.ac.ir

R. Bagheri
Materials Science and Engineering
Department, Sharif University of
Technology, P.O. Box 1136,
9466 Tehran, Iran

Abstract The morphology of a quaternary blend containing a diglycidyl ether of bisphenol-A (DGEBA), a thermoplastic modifier (PMMA), a phase-separating curing agent (diaminodiphenylmethane, DDM), and a non-phase-separating curing agent (methylenebis(3-chloro-2,6-diethylaniline, MCDEA) was studied as a function of volume fraction of the thermoplastic modifier and fractional concentration of the curing agents in their mixture. It was found that using mixtures of curing agents a co-continuous morphology could be obtained at PMMA concentrations as low as 2.5 volume percent. Using FTIR spectroscopy it was proved that specific interactions are present between PMMA and individual amine curing agents. On the other hand, there was no detectable specific interaction between PMMA and DGEBA. By analyzing the micro-indentation hardness data of the cryo-fractured samples and putting forward the "*intrinsic hardness*" concept, it was proposed that the co-continuous morphology is inherently more effective than the other morphologies in changing the mechanical properties of the above-mentioned multi-component blends.

Keywords Epoxy-thermoplastic blend · Morphology · Micro-indentation hardness · Intrinsic hardness

Introduction

Blending of existing polymers brings more opportunities for developing new useful materials. Among polymer blends, mixtures of thermosets and thermoplastics have been the focus of attention especially in the field of engineering and high-performance polymers [1, 2]. Morphology is the main controlling factor of the final properties, which can be manipulated by adjusting the enthalpic and entropic conditions of the mixture. In a reactive blend containing a thermoplastic polymer dissolved in a thermoset precursor the enthalpy and entropy of the system change continuously; this can cause a phase-separation phenomenon known as "polymerization-induced phase separation" (PIPS). The main feature of this type of phase separation is the dependence of the miscibility of the components on the conversion in addition to temperature.

Polysulfone (PSu) [3, 4, 5], poly(ether sulfone) (PES) [6, 7], polyetherimide (PEI) [8, 9, 10], poly(ether ether ketone) (PEEK) [11, 12, 13], and poly(methyl methacrylate) (PMMA) [14, 15] are the most studied thermoplastic modifiers. Rizenthaler et al. [15] did not find any specific interactions between DGEBA and PMMA. They also did not mention anything about the presence of such interactions in binary mixtures of PMMA and individual amine curing agents. Furthermore, they reported that MCDEA makes a PMMA-solubilizing network [15], whereas DDM and DDS (diamino diphenyl sulfone) formed networks containing depleted PMMA domains, 200 nm in diameter [15]. On the other hand, Rastegar et al. [14], studied inter-com-

ponent interactions in a DGEBA–DDM–PMMA blend and found specific interactions between PMMA and DDM. Furthermore, they couldn't detect any specific interactions or chemical reaction between PMMA and DGEBA even after heating the blend for several hours.

In most morphology development studies, especially in thermoplastic-modified thermosets a single curing agent (normally phase-separating) has been used [3, 4, 5, 6, 7, 8, 9, 10, 11, 12, 13]. In addition, the effect of the thermoplastic volume fraction has been studied extensively [3, 4, 5, 6, 7, 8, 9, 10, 11, 12, 13]. Notably, the thermoplastic concentration has usually been so high that the mixture processing at room temperature has been difficult or impossible.

In this research work a curing agent mixture (CAM) containing one which forms PMMA-solubilizing network and another which forms PMMA non-solubilizing network was used. Therefore, by changing the fractional volume of the curing agents in the CAM, specific composition corresponding to the formation of co-continuous morphology for various volume fractions of PMMA could be determined. Furthermore, the results of micro-indentation on blend samples were extrapolated to an infinitely low concentration of PMMA. Consequently, a new explanation for the efficacy of the co-continuous morphology in changing the mechanical properties of polymer blends was deduced.

Experimental

Materials

The epoxy resin was a liquid, solvent-free DGEBA with an epoxide equivalent weight of 175 and an average degree of polymerization of 0.15 (Epikote 828, Shell Co.). Poly(methyl methacrylate) was an injection-molding grade with a viscosity-average molecular weight of 60,000 Daltons. The curing agents were 4,4′-diaminodiphenylmethane (DDM) and methylenebis(3-chloro-2,6-diethylaniline) (MCDEA), both analytical grade from Aldrich. Tetrahydrofuran (THF) and butyl acetate were both analytical grade and supplied by Merck. All the reagents were used without further purification.

Procedures and instruments

Sample preparation

Samples for FTIR studies were cast from a THF solution on to a potassium bromide disk. After solvent evaporation, the KBr-supported film was sandwiched with another KBr disk.

Two other types of sample, thin and thick were prepared for the rest of the experiments. Thin samples were prepared by making sandwiches of predefined amounts of mixtures of components (DGEBA along with stoichiometric amount of individual amines or CAM and 2.5, 5.0, and 7.5 volume percent PMMA) between two 100-micrometer-thick cover glasses. Thick samples were prepared by casting blends into molds made of aluminium foil. Both thin and thick samples were cured for 4 h at 140°C and then for another 2 h at 200°C in a Memmert ULM 400 electrically heated oven. Thin samples, 50 micrometers in thickness, were used for light microscopy and turbidimetric studies, whereas thick samples, about 3 mm thick, were examined for appearance, fracture surface morphology, and micro-indentation hardness.

FTIR spectroscopy

The samples were studied by means of a Nicolet Magna IR 550 FTIR spectrophotometer. All the samples were scanned 32 times at a resolution of 1.0 cm^{-1} to maximize the signal to noise ratio.

Light microscopy and turbidimetric analysis

A Leica DMR (Leica AG) light microscope was used to observe the blend morphology in thin samples. The light intensity detector was used for turbidimetric analysis of the samples.

Scanning electron microscopy

The cryo-fractured samples were gold coated in a Jeol Fine Coat ion sputter JFC 1100 instrument and then viewed by means of a scanning electron microscope (ISI ABT SR-50). The electrons were shot at an energy of 20 and 25 kV.

Micro-indentation hardness

The micro-hardness tests were performed on both the fracture and the free surfaces of the samples. The samples were indented under a load of 0.9807 N, a penetration speed of 25 micrometers per second, and a dwell time of 18 seconds at room temperature by a Knoop indenter (Leica VMHT MOT).

Results and discussion

Inter-component interactions

The results of inter-components interactions studied by FTIR spectroscopy [16, 17, 18, 19] are presented in

Table 1 Shifts in the absorption bands of representative functional groups in binary blends

Binary blends	Initial wavenumber	Final wavenumber
DGEBA-PMMA		
Oxirane ring	915.84	915.8 (no broadening)
Acrylate carbonyl	1734.9	1734 (no broadening)
PMMA-MCDEA		
Acrylate carbonyl	1734.9	1734.9 (broadening)
Primary NH (asymmetric)	3396	3388.65
MCDEA-DGEBA		
Oxirane ring	915.84	916.03
Primary NH (asymmetric)	3396	3395.25
PMMA-DDM		
Acrylate carbonyl	1734.68	1727.83
Primary NH (asymmetric)	3415.36	3414.39
DDM-DGEBA		
Primary NH (asymmetric)	3414.62	3413.9
Oxirane ring	915.32	916.21

Table 1. The absorption band of the carbonyl group has either been shifted to a lower wavenumber or broadened in PMMA/DDM and PMMA/MCDEA mixtures. Also, the changes in the absorption band position of the aromatic amino group confirm the existence of specific interaction between curing agents and PMMA. On the other hand, similar interactions between curing agents and DGEBA could be deduced.

The main differences between the two amines are chlorine substitution on the phenyl rings of MCDEA and its lower reactivity [20]. Therefore the possibility of strong acid–base interactions in the MCDEA network may compensate for the repelling effect caused by the entropic frustration inserted by the network formation. Several authors [21, 22, 23, 24, 25, 26] have shown that the conformation of free chains entrapped in a polymer network will remain Gaussian up to a critical cross-link density. Above the critical cross-link density, the chain goes through a transition and takes on a localized collapsed conformation. Therefore, a soluble linear polymer in a network may acquire a more or less collapsed conformation after passing a critical cross-link density.

Turbidimetric investigations

Figure 1 shows the cloud-point curves for three DDM-cured epoxies containing different volume fractions of PMMA. The extent of conversion was controlled by using sub-stoichiometric amounts of DDM. Similar samples by MCDEA did not show any cloud point and remained completely clear for all the conversions.

As one can observe, by increasing the PMMA concentration, the substoichiometry of DDM corresponding to the cloud point decreases. On the other hand, the application of 20/80, 25/75, 30/70 and 35/65 mole fractions of DDM/MCDEA to cure a sample containing 5 volume percent PMMA did not cause any turbidity. The phase separation could be detected only when the concentration of DDM in the CAM exceeded 40 percent of

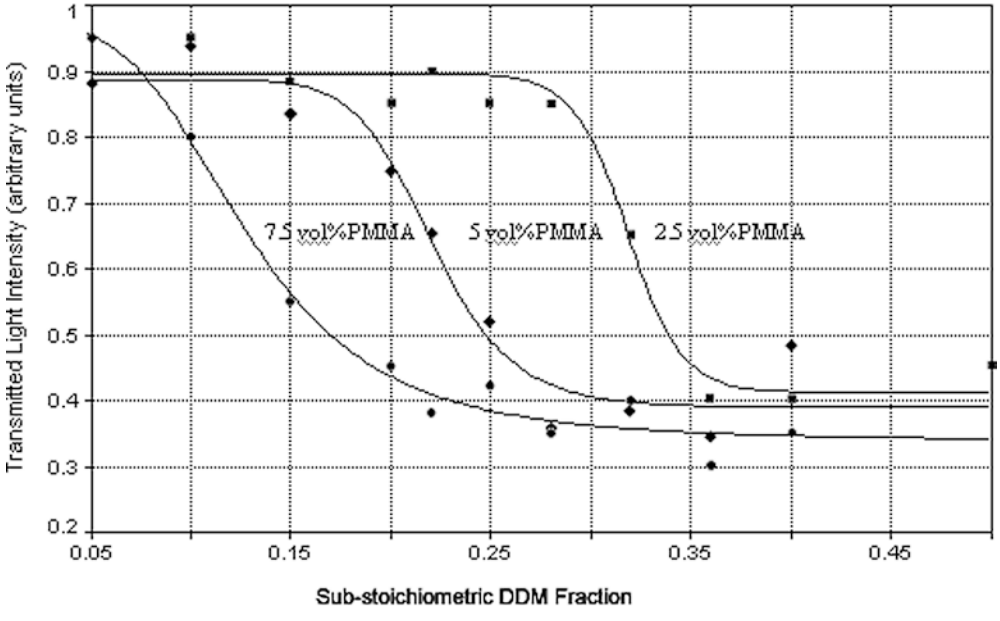

Fig. 1 The transmitted light intensity of cured samples containing different amounts of PMMA versus the sub-stoichiometric DDM fraction

its stoichiometric value. Apparently, MCDEA acts as a compatibilizer in DDM-cured epoxy-PMMA blends.

Light microscopic investigations

The kinetics and mechanisms of phase-separation in curing thermoplastic-thermoset blends have been studied by several groups [4, 17, 28, 29].

In order to capture the phase-separation phenomenon by light microscopy the blend of DGEBA and 5 volume percent PMMA was reacted with different sub-stoichiometric amounts of DDM in butyl acetate under reflux conditions. After solvent evaporation, the samples were sandwiched between thin glass slides and the light microscopic images were taken (Fig. 2).

Apparently, phase separation begins with the formation of droplet morphology, which later takes on some order (32% conversion, Fig. 2a) and becomes a co-continuous network (36% conversion, Fig. 2b). By conversion enhancement, the co-continuous network breaks down and eventually a growing droplet morphology appears (40% conversion, Fig. 2c).

Light microscopic investigations of the samples cured under solvent-free conditions showed a co-continuous morphology at much lower conversion (20%) (Fig. 3a). By increasing the conversion to 25% the co-continuous paths become finer (Fig. 3b) and finally at a conversion of 32%, the system turns to droplet morphology (Fig. 3c). The main difference of the aforementioned procedures for sample curing is the rate of the reaction. By performing the reactions in a solvent, the functional groups are diluted which leads to the expectation of lower reaction rate and phase-separation at much lower conversions. A completely different situation was observed here, however. Therefore, it seems that the higher cloud-point conversion is due to the formation of micro-gels.

Scanning electron microscopy

Figure 4 shows the scanning electron micrographs of the cryo-fractured surfaces of blends containing different volume fractions of PMMA. These samples were cured with curing agent mixtures corresponding to the co-continuous morphology. By increasing the concentration of PMMA in quaternary blends (Figs. 4A to 4C), the required DDM content of the CAM for observing a co-continuous morphology decreases from 50% to 30%. The roughest fracture surface in a series containing the same amount of PMMA was supposed to correspond to the co-continuity composition [30]. In addition, the

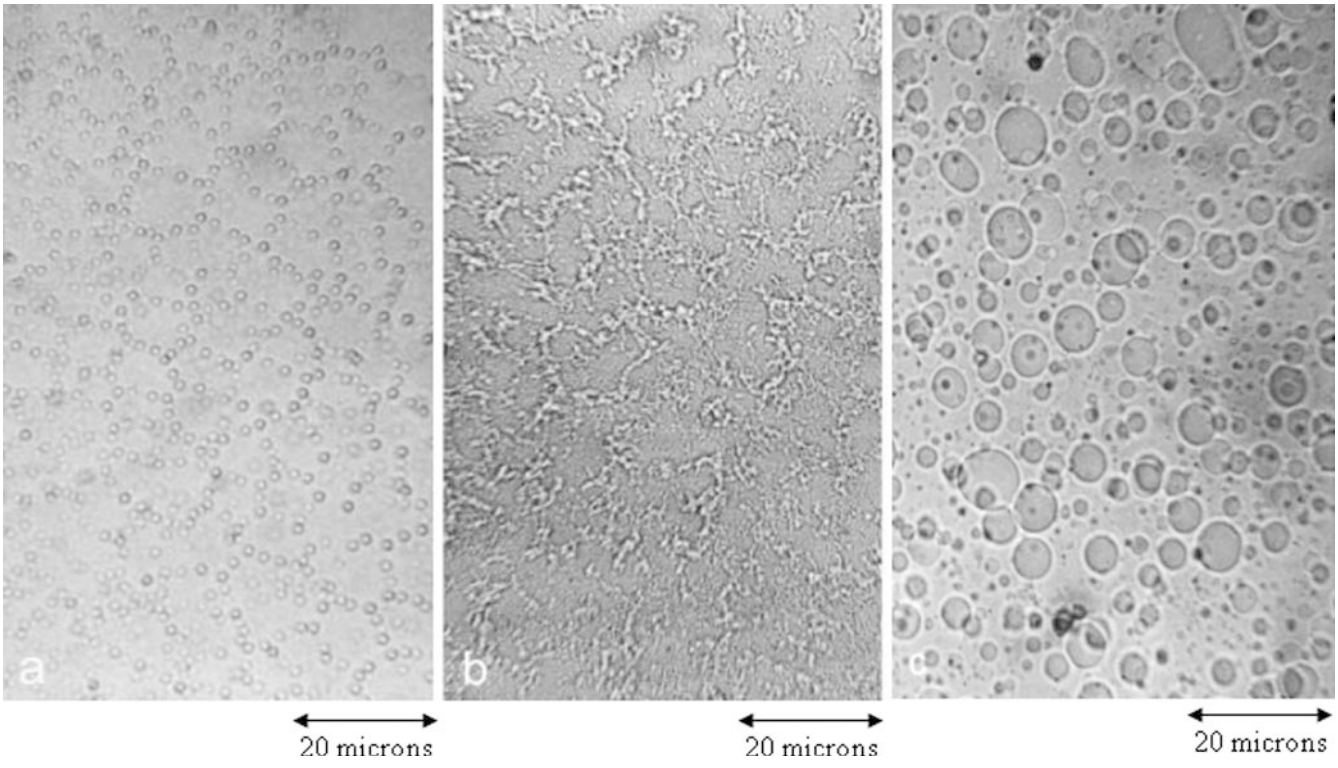

Fig. 2 Light microscopic images of different stages of phase separation in an epoxy-PMMA blend containing 5 vol% PMMA and cured with sub-stoichiometric amounts of DDM in butyl acetate reflux: (**a**) 32%, (**b**) 36%, and (**c**) 40% DDM

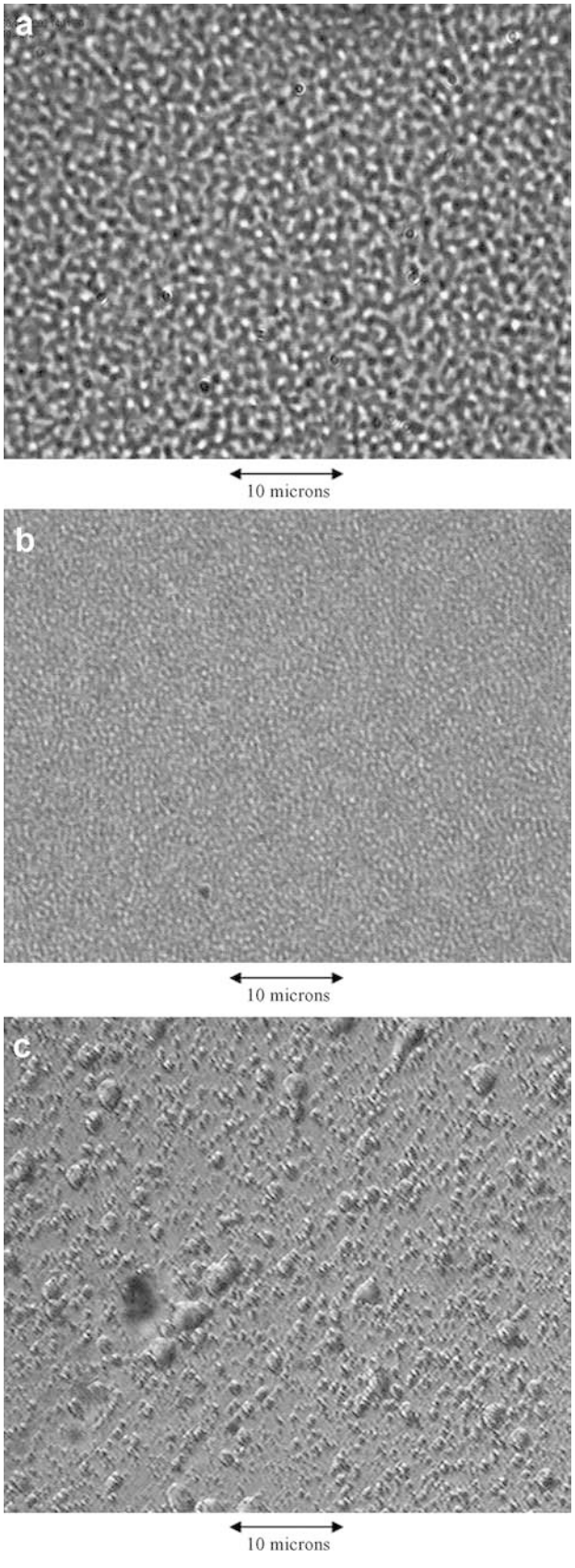

◄

Fig. 3 Light microscopic images of different stages of phase separation in an epoxy-PMMA blend containing 5 vol% PMMA and cured with DDM/MCDEA mixtures: (**a**) 20%, (**b**) 25%, and (**c**) 32% DDM

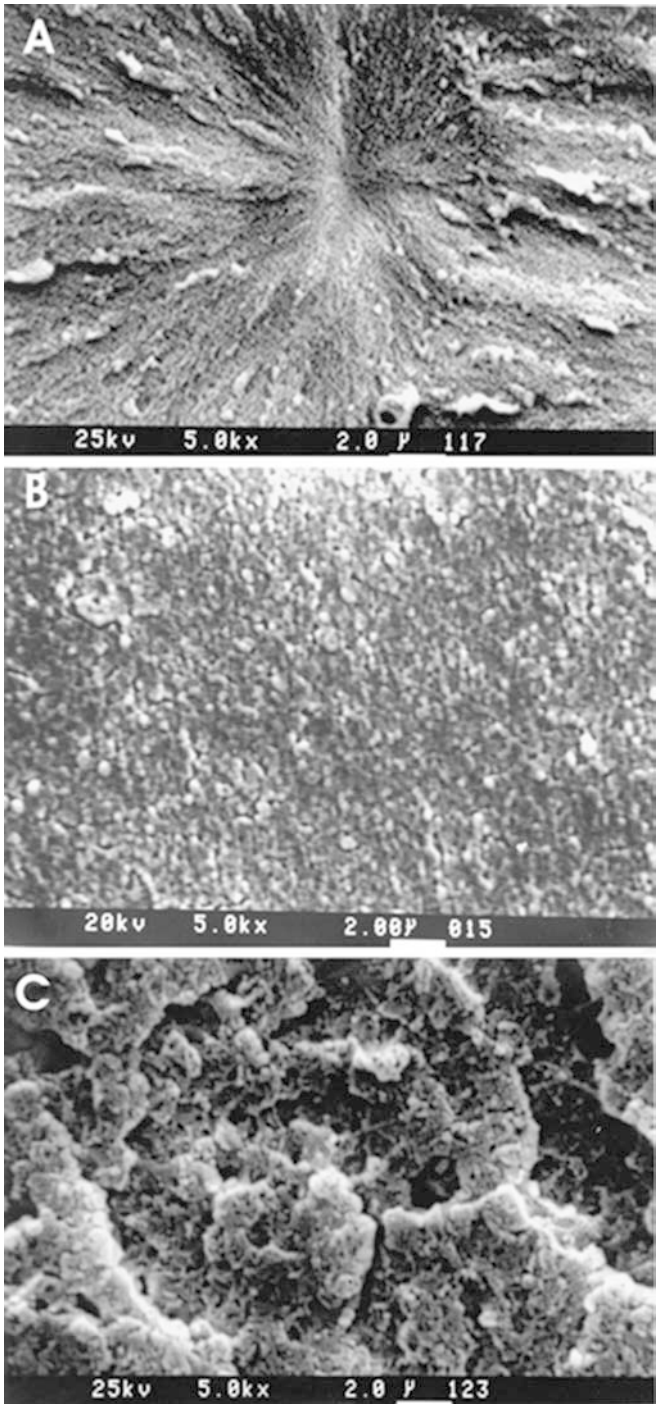

Fig. 4 SEM micrographs of the fracture surfaces of samples containing 2.5 vol% (**A**), 5.0 vol% (**B**), and 7.5 vol% (**C**) of PMMA, corresponding to the co-continuous morphologies

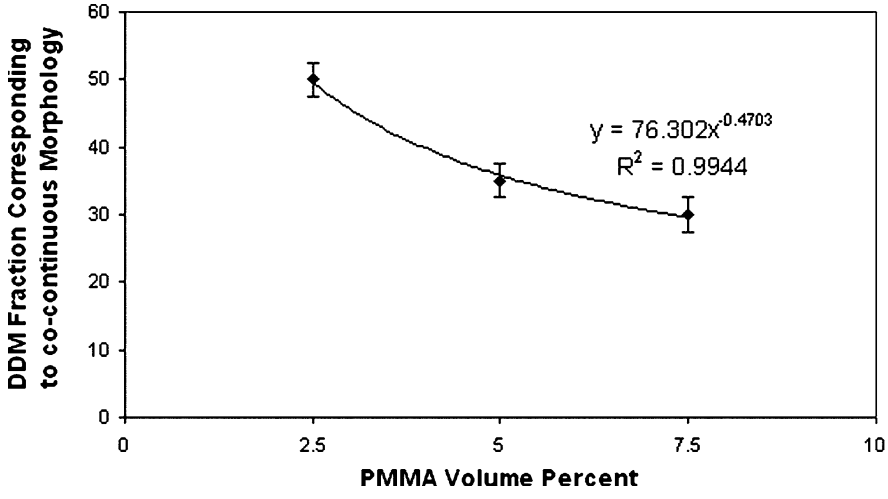

Fig. 5 Power-law relationship between the critical DDM concentration and the volume fraction of PMMA

domain size of the co-continuous network is an increasing function of the PMMA concentration. The critical DDM fraction of the CAM corresponding to the co-continuous morphology versus PMMA volume fraction is presented in Fig. 5. It seems that a power-law relationship exists between the two parameters. The power law correlation is proposed to satisfy the DDM fraction required for the co-continuous type of phase-separation at extremely low PMMA volume fractions.

Finally, it is well known that blends with co-continuous morphology are expected to show the highest fracture toughness [31]. Therefore, formation of the co-continuous morphology could be detected by mechanical tests such as micro-indentation.

Micro-indentation tests

Figure 6 shows the microscopic images of the best and the worst indentation prints observed during the measurements. For the samples with symmetrical prints three to five tries were made but for an asymmetric print an average of 10 to 12 measurements were reported. To perform crack-free indentation the Knoop indenter geometry was selected [32]. The Knoop Hardness is calculated from Eq. (1):

$$KH = \frac{1.45 \times F}{l^2} \tag{1}$$

where F and l are the load and the major diagonal of the indentation print, respectively. The hardness of the fracture surface of the samples as a function of DDM fraction in the CAM for three levels of thermoplastic is presented in Fig. 7. By increasing the DDM fraction in the CAM, the hardness of all samples decreases to a minimum and increases again.

Several authors [33, 34, 35, 36, 37, 38, 39] applied Tabor's equation [40], originally derived for metals (Eq. 2) to other materials and took into account the indenter size effect (ISE):

$$H \approx C\sigma_y \tag{2}$$

where H, σ_y and C are the sample hardness, its compressive yield stress and a material-specific constant, respectively.

The same material constant was assumed for all samples in this research. To elucidate the exclusive role of the blend morphology on its micro-hardness, the ratio of the micro-hardness of the fracture surface to that of the free surface (dimensionless hardness, DH) was evaluated (Fig. 8).

For all the concentrations of PMMA studied, the dimensionless hardness goes through a minimum as the fraction of DDM in the CAM increases. The location of the minimum for each quaternary blend depends on the volume fraction of the thermoplastic modifier, shifting to the higher DDM fraction by lowering the volume percent of PMMA (Fig. 8).

As one can see, at lower PMMA volume fractions, the dimensionless hardness at the minimum point has the lowest value. On the other hand, as the PMMA volume fraction decreases, the DDM fraction in the CAM corresponding to the co-continuity increases and finer second phase morphology is formed (Fig. 4). This can be attributed to the higher interfacial area between phases, which may enhance the effect of the low-hardness component (PMMA).

Figure 9 depicts the specific hardness, the dimensionless hardness per volume percent of PMMA, for three morphologies: single phase (MCDEA 100), droplet (DDM 100), and co-continuous as a function of the thermoplastic concentration. Surprisingly, in all cases the specific hardness values show linear variation with

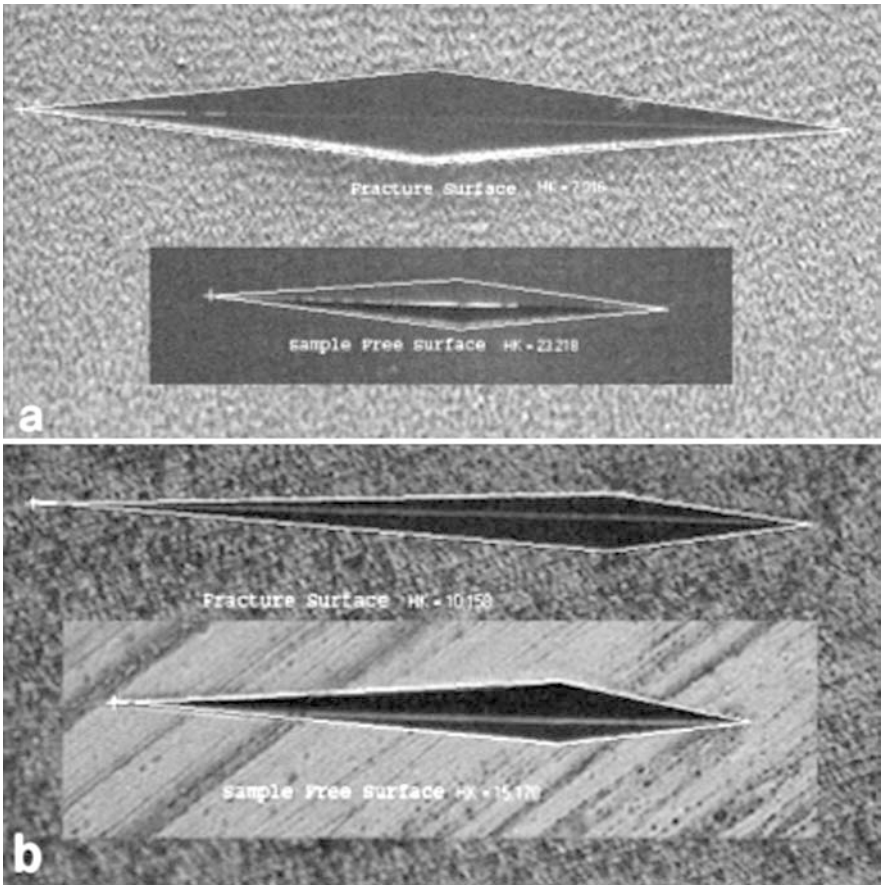

Fig. 6 The most symmetric (**a**) and asymmetric (**b**) indenter prints on the fracture and the free surfaces (*insets*) of samples containing 2.5 vol% (**a**) and 7.5 vol% (**b**) PMMA

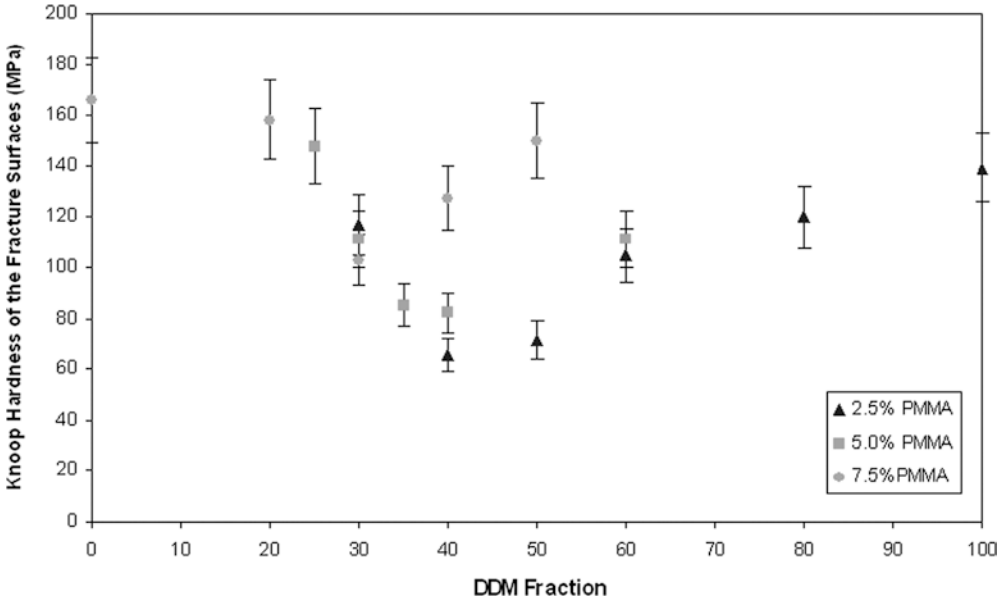

Fig. 7 Variation of the Knoop hardness of the fracture surface of the samples containing different amounts of PMMA as a function of relative DDM concentration

PMMA volume fractions. By extrapolation to zero PMMA concentration, an "intrinsic hardness" value for each type of morphology was achieved. In mathematical terms:

$$[H] = \lim \frac{DH}{\phi}_{\phi \to 0} \tag{3}$$

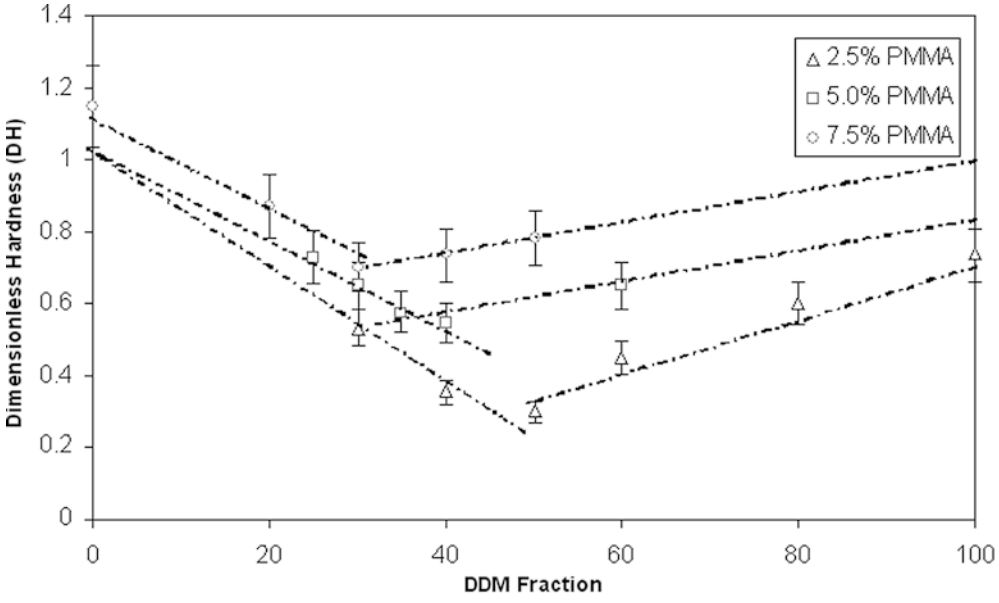

Fig. 8 Variation of the dimensionless hardness of quaternary epoxy blends with the percentage of DDM in the CAM

where $[H]$, DH and ϕ are the intrinsic hardness, the dimensionless hardness and the volume percent of the thermoplastic modifier, respectively. To clarify the term "intrinsic hardness", its comparison with the well-known "intrinsic viscosity" of polymer solutions could be fruitful. The intrinsic viscosity is a measure of the effective volume of a chain resisting flow. By comparison, the intrinsic hardness may be regarded as a measure of the effective volume of the second phase resisting compressive deformation. The intrinsic hardness values corresponding to different morphologies are tabulated in Table 2.

Krumova et al. [33] have shown that the additive law is applicable to the indentation hardness value of the polymer blends. Therefore, an "effective volume percent" for PMMA chains in three different morphologies can be calculated:

$$H_b = H_1\phi_1 + H_2\phi_2 \tag{4}$$

where, H_b, H_1, H_2, ϕ_1 and ϕ_2 are the blend hardness, hardness of components 1 and 2 and the volume fraction of the components, respectively.

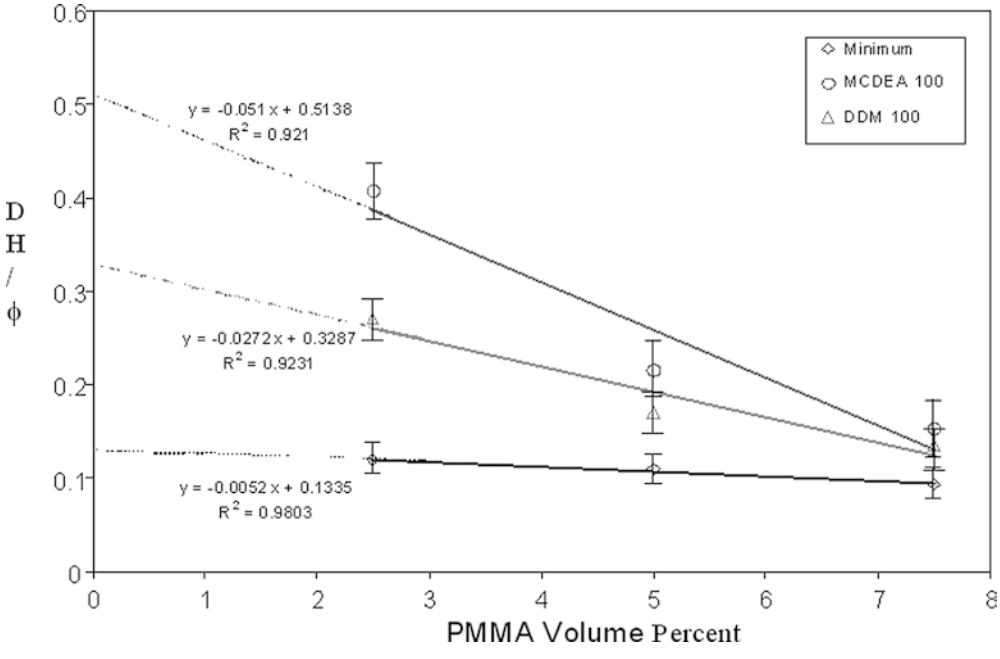

Fig. 9 Variation of the dimensionless hardness per volume percent of PMMA with the volume fraction of PMMA in quaternary epoxy blends

Table 2 Intrinsic hardness associated with different morphologies

Morphology	Intrinsic hardness
Single-phase	0.5138
Droplet	0.3287
Co-continuous	0.1335

The effective volume percent is a measure of the efficacy of the specific morphology on changing the indentation hardness of the matrix.

The effective volume percent of PMMA for the three aforementioned morphologies were approximately 2.0 for the single-phase morphology, 2.7 for the droplet morphology, and 3.5 for the co-continuous morphology. In other words, a co-continuous morphology is about 80% more efficient than a single-phase morphology in changing the hardness of the studied epoxy matrix.

Conclusion

Development of a variety of second phase morphologies in epoxy-PMMA blends cured by various fractions of DDM and MCDEA in their mixtures was studied. The results showed tuning possibilities and the need for a higher volume fraction of DDM in blends containing lower volume fraction of PMMA to achieve co-continuous morphology. The introduction of the intrinsic hardness concept revealed the higher efficacy of the co-continuous morphology in changing the properties of various blends.

Acknowledgement Extensive discussion with Dr Z. Ranjbar is highly acknowledged.

References

1. Utracki LA (1989) Polymer alloys and blends. Hanser Gardner, Munich
2. Paul DR (2000) In: Paul DR, Bucknall CB (eds) Polymer blends, vol 1. Wiley, New York
3. Xie X, Yang H (2001) Mater Des 22:70
4. Oyanguren PA, Galante MJ, Andromaque K, Frontini PM, Williams RJJ (1999) Polymer 40:5249
5. Martinez I, Martin MD, Eceiza A, Oyanguren P, Mondragon I (2000) Polymer 41:1027
6. Fernández B, Corcuera MA, Marieta C, Mondragon I (2001) Eur Polym J 37:1863
7. Di Pasquale G, Motta O, Recca A, Carter JT, McGrail PT, Acierno D (1997) Polymer 38:4345
8. Barral L, Cano J, López J, López-Bueno I, Nogueira P, Torres A, Ramírez C, Abad MJ (2000) Thermochim Acta 344:27
9. Barral L, Cano J, López J, López-Bueno I, Nogueira P, Abad MJ, Ramírez C (2000) Polymer 41:2657
10. Su CC, Woo EM (1995) Polymer 36:2883
11. Francis B, Vanden Poel Posada GF, Groeninckx G, Lakshmana VR, Ramaswamy R, Thomas S (2003) Polymer 44:3687
12. Zhikai Z, Sixun Z, Jinyu H, Xingguo C, Qipeng G, Jun W (1998) Polymer 39:1075
13. Poncet S, Boiteux G, Pascault JP, Sautereau H, Seytre G, Rogozinski J, Kranbuehl D (1999) Polymer 39:6811
14. Rastegar S, Mohammadi N, Bagheri R (2003) Proc 6th Iranian Seminar on Polymer Science and Technology, 12–15 May 2003, Tehran, Iran
15. Ritzenthaler S, Girard-Reydet E, Pascault JP (2000) Polymer 41:6375
16. Gomez CM, Bucknall CB (1993) Polymer 34:2111
17. Kuo SW, Lin CL, Chang, FC (2002) Polymer 43:3943
18. Sudhamani SR, Prasad MS, Udaya Sankar K (2003) Food Hydrocolloids 17:245
19. Rocco AM, Moreira DP, Pereira RP (2003) Eur Polym J, in press
20. Girard-Reydet E, Riccardi CC, Sautereau H, Pascault JP (1995) Macromolecules 28:7599
21. Thirumalai D (1988) Phys Rev A 37:269
22. Muthukumar M (1989) J Chem Phys 90:4594
23. Douglass JF (1988) Macromolecules 21:3515
24. Liu X, Bauer BJ, Briber RM (1997) Macromolecules 30:4704
25. Edwards S, Muthukumar M (1988) J Chem Phys 89:2435
26. Baumgaertner A, Muthukumar M (1987) J Chem Phys 87:3082
27. Chen JL, Chang FC (1999) Macromolecules 32:5348
28. Kuzub LI, Irzhak VI (2001) Colloid J 63:86
29. Williams RJJ, Rozenberg BA, Pascault JP (1997) Adv Polym Sci 128:97
30. Tanaka H (2000) J Phys Condens Matter 12:R207
31. Kinloch AJ, Young RJ (1983) Fracture behaviour of polymers. Kluwer, Dordrecht
32. Low IM, Shi C (1998) J Mater Sci Lett 17:1181
33. Krumova M, Flores A, Balta Calleja FJ, Fakirov S (2002) Colloid Polym Sci 280:591
34. Krumova M, Fakirov S, Balta Calleja FJ, Evstatiev M (1998) J Mater Sci 33:2857
35. Berthoud P, G'Sell C, Hiver JM (1999) J Phys D Appl Phys 32:2923
36. Sadeghipour K, Chen W, Baran G (1994) J Phys D Appl Phys 27:1300
37. Gauthier C, Schirrer R (2000) J Mater Sci 35:2121
38. Flores A, Balta Calleja FJ, Kircheldorf HR (1998) J Mater Sci 33:3567
39. Kourtesis G, Renwick GM, Fischer-Cripps AC, Swain MV (1997) J Mater Sci 32:4493
40. Tabor D (1951) Hardness of metals. Oxford University Press, London